JP&M Engineering
Journal of Petroleum and Mining Engineering
http://jpme.journals.ekb.eg/

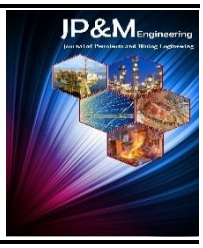

Effect of Heat Input and Shielding Gas on the Performance of 316 Stainless Steel Gas Tungsten Arc Welding

Ahmed, R.[1]*, Essa, A.R.S. [1,2], EL-Nikhaily, A. [1], Ahmed, E.[3]

[1] Mechanical Department, Faculty of Industrial Education, Suez University, Egypt.
[2] Mechanical Engineering Department, Egyptian Academy for Engineering&Advanced Technology, Affiliated to Ministry of Military Production, Egypt.
[3] Metallurgical and Materials Engineering Department, Faculty of Petroleum and Mining Engineering. Suez University, Egypt.
* ramy_fouad12@suezuniv.edu.eg & Tel: 00201017086380

Article Info

Received 27 Jan. 2020
Revised 26 Mar. 2020
Accepted 2 Apr. 2020

Abstract

The effect of nitrogen addition and heat input on weld metal microstructure and mechanical properties of 316 stainless steel is studied. Autogenous gas tungsten arc welding (GTAW) is employed by adding up to 2 vol.% N2 in Ar. Welding speed and heat input rate are measured as functions of gas composition. Weld defects are examined by radiographic testing, and weld metal microstructure is studied by optical microscopy. Mechanical properties of welds are determined by uniaxial tensile testing, hardness measurements, and bending test. Weld dendritic structure is refined by increasing N2 content in Ar. The mechanical properties and cooling rate are lower with increasing heat input. Besides, adding nitrogen to argon shielding gas leads to higher values of the ultimate tensile strength and hardness. The tensile strength, yield stress and elongation percent of welds depends strongly on the heat input and nitrogen content in shielding gas. This is discussed on the basis of microstructural characterization. Moreover, the weld nugget area, cooling time and solidification time increase with increasing heat input and nitrogen content. Finally, after applying the bending test up to 180o no cracks, tearing or surface defects could be observed on welded samples.

Keywords

Gas tungsten arc welding, nugget area, stainless steel, mechanical properties.

Introduction

Austenitic stainless steels are commonly used as structural materials, due to their good mechanical properties and high corrosion resistance. AISI 300 series is widely used in structural applications as marine exterior trim, industrial equipment as piping and super-heater tubes. It is also used for the commercial fast breeder reactor [1]. GTAW is mostly adopted for industries, which require high weld quality or precision. In GTA welding, the heat input (HI) during welding is estimated by Eq.1 [2].

$$HI\ (KJ/mm) = (V \times I \times 60) / (S*1000) \quad \text{Eq.1}$$

HI (heat input) is in KJ/mm, *V* is arc voltage in volt, *I* is welding current in Amp and *S* is welding speed in mm/min.

Shielding gas has a significant influence on the overall performance of welding. It protects the molten metal from atmospheric nitrogen and oxygen. It also promotes a stable arc and uniform metal transfer [3, 4]. The basic properties of shielding gas aids in selecting the shielding gas or gases for a welding application. Using the best gas blend improves the quality, and may reduce the overall cost of welding as well [5]. The presence of nitrogen (N_2) in the welding zone is usually due to improper protection against air. However, nitrogen is sometimes added to the inert shielding gas [6].

Nitrogen is an austenite stabilizer for austenitic and duplex stainless steels. Higher nitrogen content of weld metal decreases its ferrite content and increases the risk of solidification cracking. The influence of oxygen on nitrogen content of autogenous AISI 310 stainless steel arc welds was studied [7], and it was found that nitrogen addition to argon (Ar) shielding gas during autogenous arc welding raises the nitrogen content, but increases the possibility of active degassing and porosity. The addition of 2% oxygen to argon and argon-nitrogen shielding gas mixtures suppresses degassing and limits nitrogen-induced porosity. The influence of nitrogen and heat input on weld metal of gas tungsten arc welded high nitrogen steel “lCr21Mn16N” was studied [8]. Increasing the

addition of N_2 to Ar in the shielding gas from 2% to 10%, increases N_2 content of welds at similar heat input value. However, if N_2 content of the shielding gas is lower than some critical value, N_2 pores can be avoided. At higher N_2 contents, the tendency of porosity in weld metal increases. Also, the hardness of austenitic stainless steel welds increases with the increase of nitrogen content in weld metal [9]. Furthermore, the use of nitrogen in shielding gas increases the pitting corrosion resistance of welds [10]. Besides, the tensile strength and hardness values of austenitic stainless steel 304L welded by tungsten inert gas welding decrease with increasing heat input, but the ferrite phase, impact toughness, penetration depth, and weld bead width increase [11].

The influence of welding parameters on cooling rate and pitting resistance equivalent number (PREN) in super duplex stainless steel welds was investigated [12], and it was found that the cooling rate and grain size increase with increasing heat input. Best result for PREN is obtained using an intermediate heat input of 1.4 kJ/mm. Furthermore, it has been concluded that ultimate tensile strength (UTS) and hardness values increase with increasing welding current or heat input [13]. Highest UTS and hardness Vickers (HV) values are obtained using a current value of 100A. Also, sigma phase and $Cr_{23}C_6$ in 316 SS welded samples increase with increasing heat input.

Optimization of 316 austenitic stainless steel weld sample characteristics is carried out according to Taguchi method (analysis of variance) using the effect of welding speed, welding current, filler metal, root gap on the ultimate tensile strength and bend strength [14]. It has been concluded that the travel speed has a greater influence on toughness and the welding current has maximum influence on UTS. Furthermore, the root gaps have some effect on both tensile and bend strengths. Also, different shielding gas mixtures of pure argon containing 0%, 1%, 3%, 6%, and 9% N_2 for GTAW of 2205 duplex stainless steel [15]. It has been found that the austenitic structure increases the delta ferrite decreases with increasing nitrogen content. The weld nugget area increases with increasing the welding current and arc voltage, and decreases with increasing the welding speed [16], and the weld nugget area can be calculated with empirical Eq.2.

$$Na = 33.312 * 10^{-6} * [A^{1.55} / S^{0.903}] \quad \text{Eq.2}$$

Where, Na is the nugget area in mm2, A is welding current in Amp, and S is the welding speed in mm/sec.

The cooling rate is the temperature loss per unit time, and in the range 800 to 500oC it is important for the phase transformation of stainless steel, and it plays an important role in determining the final microstructure of weld metal and its properties [17]. The cooling rate and cooling time can be calculated with Eq.3 and Eq.4 [18, 19], respectively.

$$\left(\frac{\partial T}{\partial t}\right)_x = \left(\frac{\partial T}{\partial x}\right)_t \times \left(\frac{\partial x}{\partial t}\right)_T = -2\pi K \times \left(\frac{(T - T_o)^2}{H_{net}}\right) \quad \text{Eq.3}$$

$$t_{8/5} = \frac{HI}{2\pi\lambda} \times \left(\frac{1}{500 - T_o} - \frac{1}{800 - T_o}\right) \quad \text{Eq.4}$$

Where, $(\partial T/\partial t)_x$ is the cooling rate in ℃/sec, K or λ is the thermal conductivity in W/mm.K, and T is the temperature near pearlite nose on the TTT diagram at 550℃ and T_o is the initial welded plate temperature (20℃).

The solidification time (S_t) of the welding joint depends on cooling rate and heat input. Hence, S_t affects the microstructure and properties of the joint, and the solidification time can be calculated by Eq.5 [20]:

$$S_t = L\, H_{net} / 2\pi k \rho_c (T_m - T_o)^2 \quad \text{Eq.5}$$

Where, S_t is solidification time in sec, L is the heat of fusion in J/mm³ (is 2 J/mm³ for steel), H_{net} is heat input, ρc is volumetric specific heat in J/mm³.℃, and T_m is the melting temperature in ℃. The influence of welding speed on mechanical properties in 304L stainless steel welds was investigated [21], and it was found that the mechanical properties and cooling rate increase with increasing welding speed. Best result for mechanical properties is obtained using an intermediate welding speed of 1.5 m/min.

Present study is concerned with evaluating the mechanical properties and weld defects of AISI 316 stainless steel using different volume ratios of nitrogen in argon shielding gas and different heat input values.

Experimental Work

Present welding material is 4 mm thick commercial 316 austenitic stainless steel. The chemical compositions of the steel and filler metal used are given in Table 1, and the mechanical properties of base metal and filler metal are measured using Instron uniaxial tensile machine at a strain rate of 10-3 s-1, as shown in Table 2.

Table 1 Typical chemical composition of 316 SS and nominal chemical composition of welding wire ER316L [22].

Composition	C	Cr	S	Mn	Mo	Ni	P	Si	Fe
316 SS	0.08	16-18	0.03	2.0	2-3	10-14	0.045	1.0	Balance
ER316L	0.04	17-20	0.03	0.5-2.5	2-3	11-14	0.040	1.0	Balance

Table 2 Mechanical properties of 316 SS and welding wire ER316L [22].

Property	UTS	Yield Strength	Elongation
SS 316	515 MPa	205 MPa	40 %
ER316L	480 MPa	170 MPa	40 %

GTA welding is carried out on 316 SS samples; 200 mm long, 100 mm wide and 4 mm thick. The detailed parametric combinations used in the present study are presented in Table 3, and the butt joint is prepared with a root face of 2 mm. Welds and shielding gas mixture are carried out in the workshop of Petrojet Company, on GTAW machine (CEA Top 250 HF) for research and development.

Table 3 Gas tungsten arc welding parameters.

Parameter	Value	Parameter	Value
Welding process	GTAW (Manual)	Shielding gas	Pure argon and Ar-2%N_2
Welding configuration	Butt joint	Polarity	DC negative electrode
Welding wire	ER316L	Welding current	80, 100 and 130 Amp

Different shielding gas compositions are used in present work following the requirements of ASME SFA 5.32: Pure argon and 98%Ar-2%N2. The radiography testing (RT) is carried out in the Petrojet Company (DELTA 800).

Vickers hardness profile through the transverse cross section of the weld joint is determined by measuring the hardness every 1 mm using a single line of indentations with 1 kg load and 20 sec loading time.

The microstructure of as-welded joints and the fracture surface of broken samples under tensile testing are characterized with optical microscope. The metallography of weldments is carried out by applying the conventional technique. Polished samples are etched in a solution of 15 ml HCL, 10 ml HNO3, and 10 ml CH3COOH for 10 sec.

The yield stress and ultimate tensile strength are determined by a universal testing machine (Instron Model, 4208-002) at a strain rate of 10-3s-1. The dimensions of the standard tensile sample (ASTM E8), are shown in Figure 1.

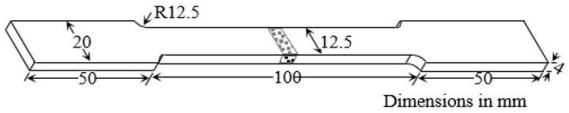

Figure 1 Geometry of standard tensile test specimen.

To determine the deformability of the welded steel, bending test according to ASTM E190-92 is applied. The specimen is put on two supporting rollers and a former is pressed through the rollers. The distance of supporting rollers is Lf = d + 3a (former diameter + three times specimen thickness). If a surface crack on specimen backside develops, the test is stopped and the bending angle is measured.

Results and Discussion

GTAW butt joints are processed using two different shielding gas mixture; pure argon and Ar-2%N_2, and using also different heat input values. After welding, visual inspection showed no surface defects such as cracks and porosity.

Weld joints are radiographic tested to trace any internal defect as porosity, internal cracks or inclusions. Weld image is captured by an X-ray camera located above the specimen at a particular distance. Radiographic images indicated that a sound internal structure without porosity or cracks is obtained using pure Ar or Ar-2%N2 as shielding gas, as presented in Figure 2.

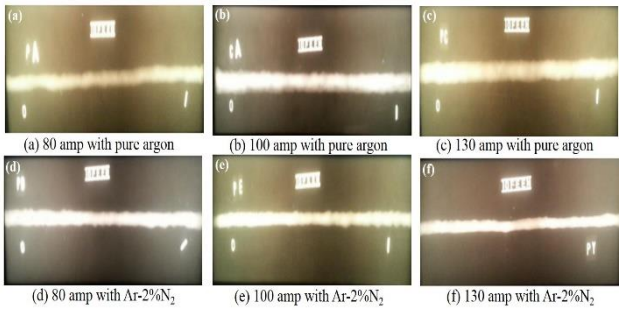

Figure 2 Radiographic test films of GTAW weldments of AISI 316 SS.

Heat input 'HI', cooling rate 'ϑT/ϑt', cooling time 't8/5'and solidification time 'St' during and after welding are important to determine samples behaviour, and are calculated by equations Eq.1, Eq.3, Eq.4 and Eq.5, respectively [2,18-20]. Heat input increases with increasing welding current and arc voltage but decreases with increasing welding speed, as presented in Fig.3. The cooling rate decreases with increasing heat input, as shown in Fig.4. Besides, the cooling time and solidification time increase with increasing welding current, as shown in Fig.5 and Fig.6, respectively. Besides, t8/5 and St decrease with increasing the welding speed.

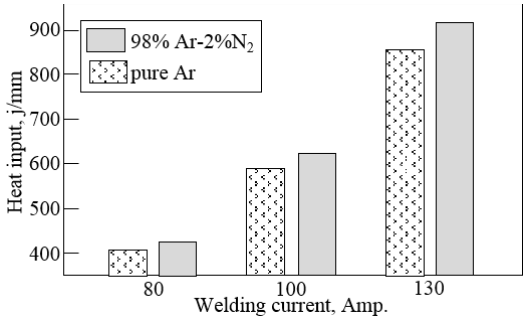

Figure 3 Heat input of welding 316 SS using 2 shielding gases and 3 weld current values.

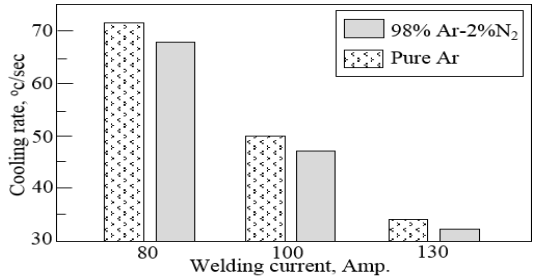

Figure 4 Cooling rate of welding 316SS using 2 shielding gases and 3 weld current values.

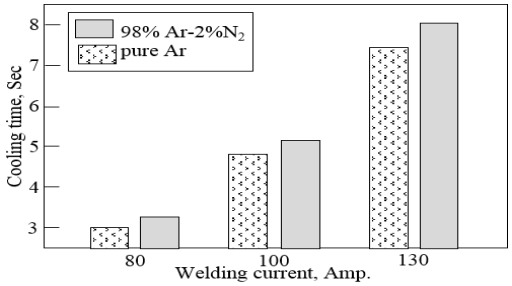

Figure 5 Cooling time of welding 316SS using 2 shielding gases and 3 weld current values.

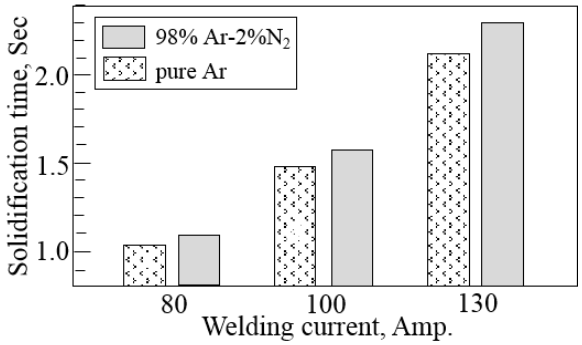

Figure 6 Solidification time of welding 316SS using 2 shielding gases and 3 weld current values

Fig.7 shows the weld nugget of a square shaped weld joints under different shielding gases and heat input for 316 SS joints. The weld nugget area increases with increasing heat input (welding current) and N2 content in the shielding gas. Besides, it decreases with increasing welding speed. Increasing the welding current leads to a wider cross-sectional area of all weld joints. Hence, increasing heat input increases the depth and width of fusion weld metal, as shown in Fig.7b. Also, the penetration and cross-sectional area of weld metal increases with increasing nitrogen content of shielding gas. Nitrogen addition to argon increases heat input. This increases heat transfer from the arc into the specimen, and produces deeper weldments. This agrees with previous reports [15, 16], that specimen width increases with increasing heat input and nitrogen content of shielding gases.

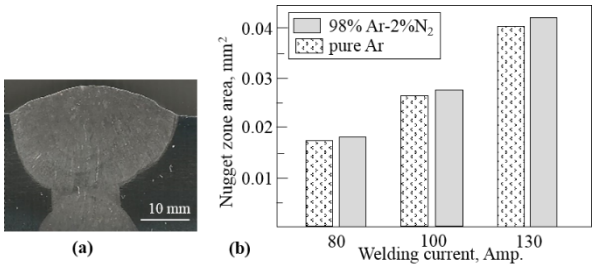

Figure 7 Macrostructure of weld specimen, b) Nugget area of welding 316 SS using 2 shielding gases and 3 welding current values.

Microstructure of base metal is fully austenitic with well-defined grain boundaries. Average grain size is about 66.0712 ± 3.05 µm as measured by the linear intercept method (ASTM E112), Fig.8. Microstructures of weld joints using pure argon or Ar and 2%N2 as shielding gases and different values of welding current are presented in Fig.9 and Fig.10, respectively. The microstructures in Fig.9b and Fig.10b are in other locations than those in Fig.9a, and Fig.10a. The heat affected zone and fusion zone are identified easily. Grain size in the weld zone increases with increasing heat input. It is known that increasing heat input decreases the cooling rate of weld metal [11]. The welding temperature is above the austenite transformation temperature and the grains grow to form overheated coarse grain structure. Fine grain regions are formed, due to the higher cooling rate of the base metal. In the incomplete recrystallization zone, since only some of the metal recrystallizes, various grain sizes are formed. The welding microstructure changes from dendritic to columnar dendritic and then to dendritic structure [13].

The addition of nitrogen to argon increases heat input, and coarsening of dendrites, due to the increase of the arc voltage [11, 23]. Fig.11 shows comparable between microstructures of weld zone with/without N2 with various welding current. Hence, the weld metal temperature increases, and a deeper weld penetration is obtained. It is interesting to observe that the microstructural features of the weld metal are significantly influenced by nitrogen content of the shielding gas. Delta ferrite content in the weld zone decreases with increasing N2 content. This agrees with previous observations [4].

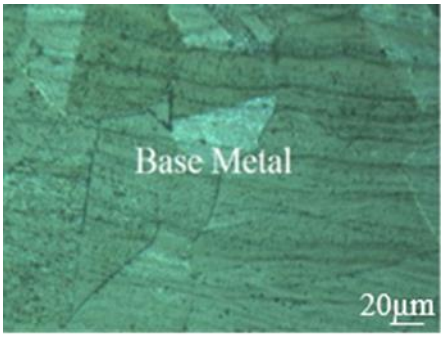

Figure 8 Microstructure of base metal.

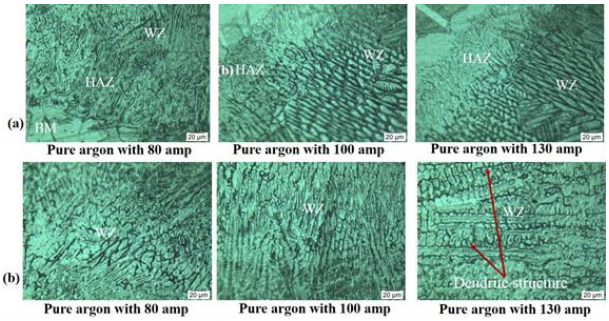

Figure 9 Microstructure of weldments using various welding currents 80, 100 and 130 Amp and pure argon as shielding gas, at different locations (a) and (b).

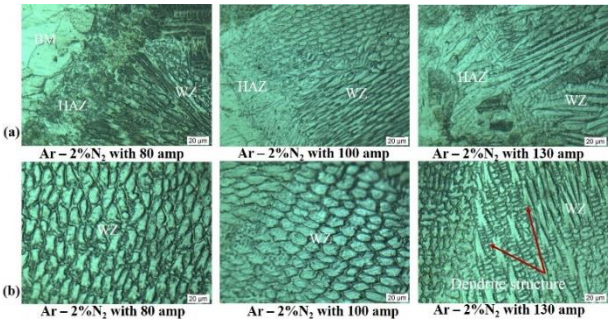

Figure 10 Microstructure of weldments using various welding currents 80, 100 and 130 Amp and Ar-2%N2 as shielding gas, at different locations (a) and (b).

The tensile test is applied to evaluate strength and plasticity of welding joints and to examine the influence of welding defects. The ultimate tensile strength and yield stress of GTAW welding joints are presented in Fig.12 and Fig.13. The tensile strength of base metal is much lower than that of all welding samples. The UTS and YS of welding samples increase with increasing nitrogen content in shielding gas, and

decrease with increasing HI. Increasing HI leads to grain size increase in the weld region that is consistent with the hardness results. Applying low heat input (80 Amp) and Ar-2%N2 shielding gas leads to maximum UTS and YS values, and minimum UTS and YS values are obtained for the base metal.

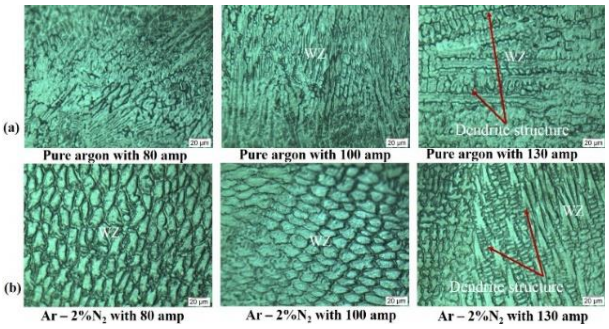

Figure 11 Microstructure of weldments using various welding currents 80, 100 and 130 amp with/without N_2.

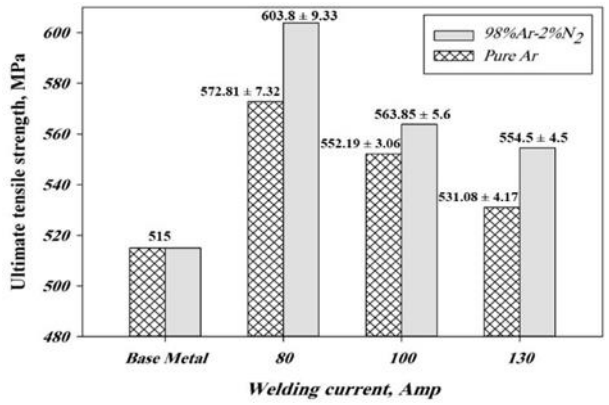

Figure 12 Ultimate tensile strength of GTAW welded AISI 316 SS using various welding currents 80, 100 and 130 Amp and Ar-2%N2 as shielding gas.

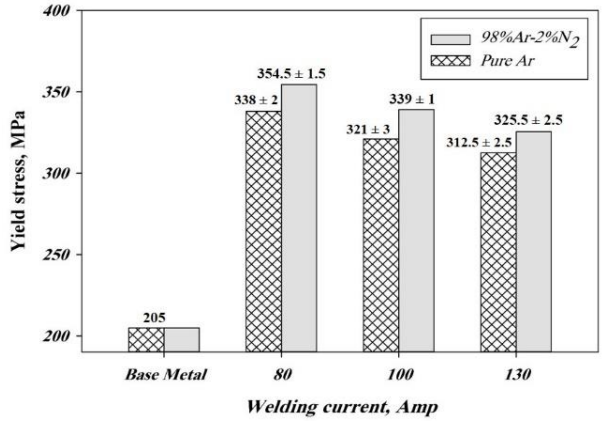

Figure 13 Yield stress of GTAW welded AISI 316 SS using various welding currents 80, 100 and 130 Amp and Ar-2%N2 as shielding gas.

Percentage elongation (EL%) of GTA welded joints are presented in Fig.14, as calculated by subtracting the length obtained after breaking and the gauge length. The elongation percent decreases with increasing welding current that is consistent with results of the UTS and YS.

The hardness is measured and plotted in Fig.15 and Fig.16 (ASTM E384-09) to show the hardness variation at various weldment locations, as weld zone (WZ), heat affected zone (HAZ) and base metal (BM). The hardness values in the HAZ and BM is greater than in the weld zone, because the grain size in the weld zone increases with increasing heat input. Increasing heat input leads to decreasing the cooling rate of weld metal. Hardness distribution on weldment cross-section of 316 SS specimens welded using different heat input values and pure argon shielding gas. The hardness decreases with increasing heat input. Furthermore, nitrogen addition to argon shielding gas leads to hardness increase. Fig.17 shows comparable between hardness values with/without N2 at various welding current. Highest hardness value is obtained in specimens using Ar-2%N2 shielding gas and 80Amp welding current, which is in agreement with previous observations [11, 13].

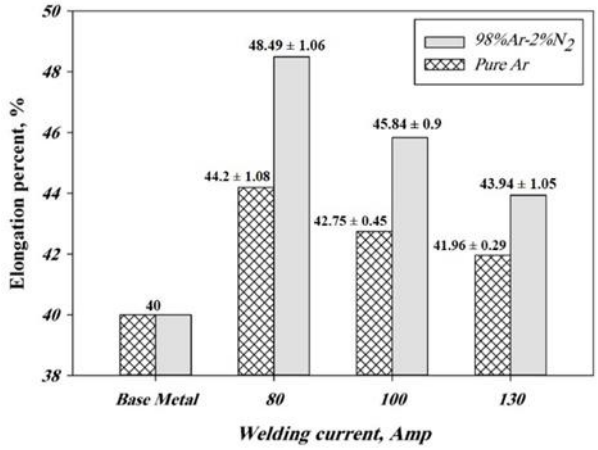

Figure 14 Percentage elongation of 316 SS welding specimens.

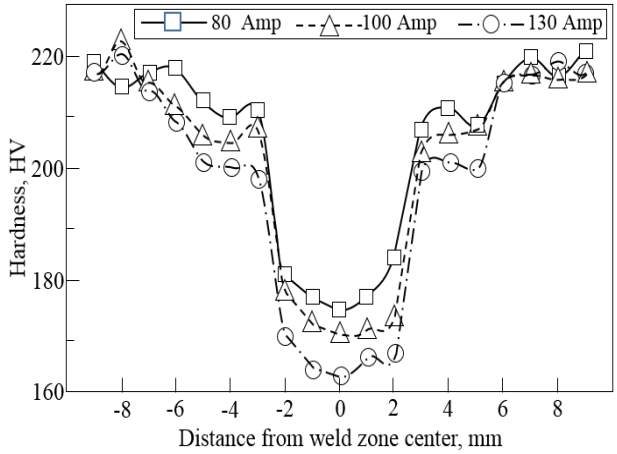

Figure 15 Hardness profiles of 316 SS GTAW joint cross sections of weld joints using pure argon as shielding gas.

Bending test (root bend test and face bend test) is applied up to 180o. After visual examination of bent samples, no tearing, cracks or any other bending defects could be observed, Fig.18.

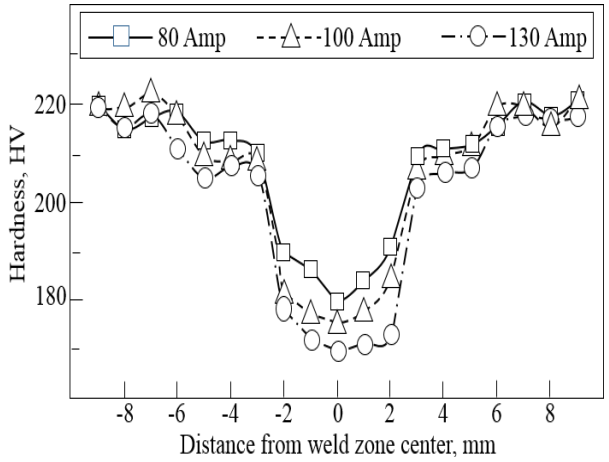

Figure 16 Hardness profiles of 316 SS GTAW joint cross sections of weld joints using Ar-2% N2 as shielding gas.

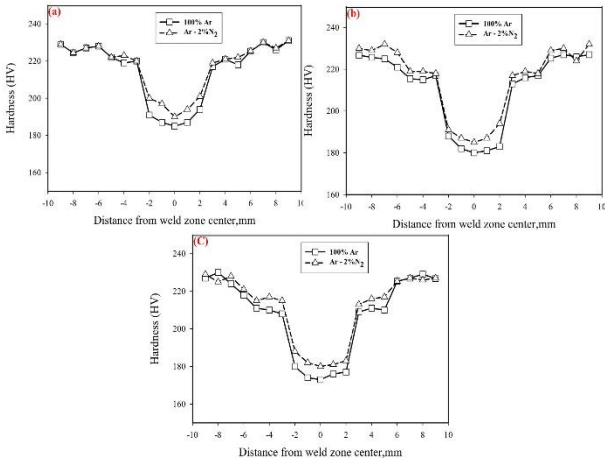

Figure 17 Hardness values of 316 SS GTAW joint cross sections of weld joints using various welding current, (a) 80, (b) 100 and (C) 130 amp with/without N_2.

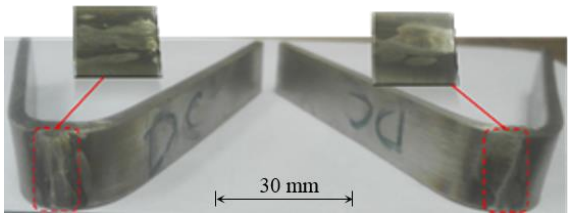

Figure 18 Bending test of welding specimens using Ar-2%N2 shielding gas and 80 Amp welding current.

Conclusions

Gas tungsten arc welding of 316 austenitic stainless steel is studied using pure argon and Ar-2% N2 as shielding gases. The following conclusions could be drawn:

- The addition of 2% N_2 content to Ar as shielding gas leads to higher UTS than using pure Ar. This addition leads to enhancement of UTS 15.43% compared with base metal at 80 amp. On the other hand, the shielding gas without N_2 the UTS enhancement is only 9.61%.
- The UTS, YS and EL% decrease with increasing heat input, and the addition of 2%N_2 to Ar shielding gas increases the mechanical properties of 316 stainless steel weld joints. The best mechanical properties are obtained at welding current 80 amp with Ar-2%N_2.
- The hardness is lower in the weld zone than in the heat affected zone and base metal, and the addition of 2% N_2 to shielding gas increases it. Moreover, the hardness decreases with increasing heat input (welding current).
- After applying the bending test up to 180^o on welding specimens, no cracks, tearing or surface defects could be observed by visual inspection.
- Heat input, cooling time, solidification time and nugget area increase with increasing the welding current. Besides, the cooling rate decreases with increasing the welding current.

Acknowledgements

The authors are deeply acknowledged the Petrojet Company (Suez Branch, Egypt) for providing welding process and collaboration.

Nomenclature

AISI	= American Iron and Steel Institute
Ar	= Argon
ASTM	= American Society for Testing Material
E%	= Elongation%
GTAW	= Gas Tungsten Arc Welding
HAZ	= Heat Affected Zone
HV	= Hardness Vickers
PREN	= Pitting Resistance Equivalent Number
RT	= Radiographic Test
SS	= Stainless Steel
TTT	= Time Temperature Transformation
UTS	= Ultimate Tensile Strength
YS	= Yield Strength

References

[1] Joseph Ki, Leuk L., Shek C.H., Lo K.H., "Stainless Steels: An Introduction and Their Recent developments," Bentham Science Publishers, 2012, p. 23-40.

[2] Dilip Kumar Singh, Gadadhar Sahoo, Ritwik Basu, Vikram Sharma and M.A. Mohtadi-Bonab, "Investigation on the microstructure-mechanical property correlation in dissimilar steel welds of stainless steel SS 304 and medium carbon steel EN 8," Journal of Manufacturing Processes, vol. 36, 2018, p. 281-292.

[3] Srinivasan K., Balasubramanian V., "Effect of Heat Input on Fume Generation and Joint Properties of Gas Metal Arc Welded Austenitic Stainless Steel," International Journal of Iron and Steel Research, vol. 18, no.10, 2011, p. 72-79.

[4] Muñoz A. I., Antón J., Guiñón J. L. and Herranz V. P., "Effect of Nitrogen in Argon as a Shielding Gas on Tungsten Inert Gas Welds of Duplex Stainless Steels," Nace International, vol. 61, no. 7, 2005.

[5] Lyttle, K.A., "ASM Metals Handbook, Welding, Brazing, and Soldering," vol. 6, ASM International, USA, 2011.

[6] Mostafa Abdelmotteleb, Mohamed R. El-Koussy and, Nahed A. Abdel Raheem, "Effect of Shielding Gases on Mechanical and Corrosion Prpperties of Steel 316L

Using FCAW," Faculty of Engineering, Cairo University, 2015.

[7] Du Toit, M., and Pistorius, P.C., "The Influence of Oxygen on the Nitrogen Content of Autogenous Stainless Steel Arc Welds," Welding Journal, vol. 86, 2007, p. 222-230.

[8] Lin, Z., Zhi-ling, T., Yun, P., Yan-chang, Q., and Yan-jie, W., "Influence of Nitrogen and Heat Input on Weld Metal of Gas Tungsten Arc Welded High Nitrogen Steel," International Journal of Iron and Steel Research, vol. 14, no. 5, 2007, p. 259-262.

[9] Chou, C.P., and Tseng, K.H., "The Study of Nitrogen in Argon Gas on the Angular Distortion of Austenitic Stainless Steel Weldments," Journal of Materials Processing Technology, 2003, p. 139-144.

[10] Bhatt, R.B., Kamat, H.S., Ghosal, S.K., and De, P.K., "Influence of Nitrogen in the Shielding Gas on Corrosion Resistance of Duplex Stainless Steel Welds," Journal of Materials Engineering and Performance, 1999, p. 591-597.

[11] Mosa. E. S., Morsy. M. A. and Atlam. A., "Effect of Heat Input And Shielding Gas on Microstructure and Mechanical Properties of Austenitic Stainless Steel 304L," International Research Journal of Engineering and Technology (IRJET), vol. 4, no. 12, 2017, p. 370-377.

[12] Huei-Sen Wang, "Effect of Welding Variables on Cooling Rate and Pitting Corrosion Resistance in Super Duplex Stainless Weldments," Materials Transactions, The Japan Institute of Metals, vol. 46, 2005, p. 593-601.

[13] Navid Moslemi, Norizah Redzuan, Norhayati Ahmad and Tang Nan Hor, "Effect of Current on Characteristic for 316 Stainless Steel Welded Joint Including Microstructure and Mechanical Properties," 12th Global Conference on Sustainable Manufacturing, vol. 26, 2015, p. 560-564.

[14] Bharatha. P., Sridharb. V.G. and Senthil kumarb. M, "Optimization of 316 Stainless Steel Weld Joint Characteristics using Taguchi Technique," Procedia Engineering, vol. 97, 2014, p. 881-891.

[15] Aziz Barıs Basyigit and Adem Kurt , "The Effects of Nitrogen Gas on Microstructural and Mechanical Properties of TIG Welded S32205 Duplex Stainless Steel," Metals, vol. 8, no. 226, 2018, p. 1-13.

[16] Shultz. B. L. and Jackson. C. E. "Influence of Weld Bead Area on Weld Metal Mechanical Properties," Welding Research Supplement, 1973, p. 1-13.

[17] Debasish Das, Dilip Kumar Pratihar and Gour Gopal Roy,"Cooling Rate Predictions and its Correlation with Grain Characteristics During Electron Beam Welding of Stainless Steel," The International Journal of Advanced Manufacturing Technology, vol. 97, 2018, p. 2241-2254.

[18] Merchant Samir Y, "Investigation on Effect of Heat Input on Cooling Rate and Mechanical Property (Hardness) of Mild Steel Weld Joint by MMAW Process," International Journal Of Modern Engineering Research (IJMER), vol. 5, no. 3, 2015, p. 34-41.

[19] Oystein Grong, "Metallurgical Modelling of Welding" The Institute of Materials, London, vol. 2, 1994, p. 1-70.

[20] Charlotte Weisman, "Welding Handbook, Fundamentals of Welding," American Welding Society, Miami, Florida , vol. 1, no. 9, 1976, p. 84-89.

[21] Sung-Min Jung, In-Duck Park, Kwang-Hyeon Lee, Jeong Suh, Gong-Young Kim and Ki-Woo Nam, "Study on Mechanical Properties of Austenitic Stainless Steel Depending on Heat Input at Laser Welding," Journal of Mechanical Science and Technology, vol. 34, 2020, p. 117-126

[22] John C. Lippold, and Damian J. Kotecki, "Welding Metallurgy and Weldability of Stainless Steel," Wiley-VCH, 2005, p. 141-152.

[23] Nabavi B., Goodarzi M. and Amani V., "Nitrogen Effect on the Microstructure and Mechanical Properties of Nickel Alloys", Welding Journal, vol. 94, 2015, p. 53-60.